

Destruction of superconductivity in the narrow-band metal K_3C_{60}

Susan K. Watson, Kimberly Allen, D. W. Denlinger, and F. Hellman
University of California San Diego, La Jolla, California 92093

(Received 24 October 1996)

Transport data on K_3C_{60} prepared with different amounts of disorder are presented, indicating that as the disorder is increased the material undergoes a superconductor-insulator transition, a result which does not occur in conventional wide-band metals. We speculate that this behavior is a consequence of the narrow conduction band and low electron density in K_3C_{60} , which gives rise to an extreme sensitivity to disorder and correlation effects. [S0163-1829(97)06206-1]

Disorder and electron correlations can have profound effects, changing the ground state of a material from metallic to insulating [referred to as a metal-insulator (M-I) transition].¹ The disorder creates localized states at the band edges. By varying the composition of a material, the Fermi energy E_F can be swept from a region of extended states at midband into a region of localized states. Alternatively, one can imagine studying the effects of introducing disorder at *fixed* composition. For conventional three-dimensional (3D) wide-band metals or superconductors, where E_F lies at midband, disorder causes only minor, albeit important effects.² Although disorder decreases the electron mean free path, and electron correlations affect the temperature dependence of the resistivity, the conductivity $\sigma(T)$ extrapolated to zero temperature, remains nonzero. In ion-damaged Nb_3Sn , for example, the magnitude of the resistivity increases and the superconducting transition temperature decreases with increasing disorder;³ the temperature coefficient of resistivity changes from positive to negative at $\rho(300\text{ K}) \approx 100\ \mu\Omega\text{ cm}$, a characteristic value for metallic glasses. In spite of these changes, Nb_3Sn remains superconducting even when it is amorphous.

In fact, there is no known homogeneous 3D superconductor where it is generally agreed that it has been driven insulating by disorder alone. For most materials, the width of the conduction band is so much larger than the potential fluctuations due to disorder that localized states appear only at the band edges, far from E_F . In addition, screening is usually sufficient to reduce correlation effects. Instead, the M-I transition is typically studied in 3D by varying composition, which changes E_F . For 3D amorphous Nb_xSi_{1-x} , for example, as the Nb concentration is reduced from 20 to 10 at. %, the material evolves continuously from superconducting to metallic [$\sigma(T \rightarrow 0) \neq 0$] to insulating [$\sigma(T \rightarrow 0) = 0$]. At the transition, tunneling data indicate that the density of states at E_F is suppressed by correlation effects.⁴ Granular systems such as Al have been driven insulating by disorder, but this material is macroscopically inhomogeneous, containing regions of Al separated by insulating Al oxide which presumably become intermingled. It has also been claimed that InO_x undergoes an insulator to superconductor transition upon annealing the disordered insulator, but with the caveat that there is no known well-defined InO_x superconductor (and, in fact, ordered InO_x is an insulator), raising the possibility that the observations are related to precipitation of a percolating path of In, a known superconductor. In 2D,

where the consequences of disorder are much greater, there are well known examples of systems driven insulating by disorder alone, both conventional metals and the high- T_c superconductors, generally considered to be dominated by the 2D nature of the CuO planes.

In this paper we will demonstrate that K_3C_{60} , although a 3D metal and superconductor when the lattice is ordered,⁵ undergoes a transition to an insulating state with increasing disorder. In many respects K_3C_{60} is an unconventional metal. Due to weak van der Waals bonding between C_{60} molecules, the conduction band is narrow, $\approx 0.5\text{ eV}$,⁶ an order of magnitude smaller than conventional metals. Electron correlations are significant, with a correlation energy on the order of 1.0–1.8 eV.^{7,8} The electron density in K_3C_{60} is low [$4 \times 10^{21}\text{ cm}^{-3}$ (Ref. 9)] making screening less effective than in conventional metals. The room-temperature resistivity of K_3C_{60} , $\approx 1.5\text{ m}\Omega\text{ cm}$, is four times larger than the Ioffe-Regel limit, implying a mean free path shorter than the intermolecular spacing. The resistivity, which should saturate near the Ioffe-Regel limit, does not appear to do so up to $\approx 800\text{ K}$ in K_3C_{60} .¹⁰ The short mean free path and lack of resistivity saturation have led to suggestions that A_xC_{60} (A alkali) belongs to a class of materials to which the independent electron picture does not apply and to which new concepts for both the normal and superconducting states must be developed.^{11,12}

A_xC_{60} forms a series of line compounds with stable phases at $x=0,1,3,4,6$ (0 is the empty band; 6 is filled).⁵ In the standard growth technique, a C_{60} film is grown first and the alkali is subsequently deposited and annealed above room temperature (typically $\leq 200\text{ }^\circ\text{C}$), diffusing into interstitial sites of the lattice. A film grown at other x will phase separate into a mixture of stable phases. Below room temperature, however, the ability of potassium to diffuse is significantly reduced and metastable phases or compositions may be trapped.

Samples in this study are prepared by codeposition of K and C_{60} , which ensures mixing even at low deposition temperatures. K_xC_{60} films, which are air sensitive, are grown and measured in an ultrahigh vacuum environment using well-degassed K (SAES Getters) and C_{60} (MER Corp., 99.9% pure). Typical base pressure is 2×10^{-10} Torr and 5×10^{-8} Torr during growth. The substrates, amorphous silicon nitride-coated Si, are mounted at the end of a copper cold finger of a He cryostat. Two radiation shields, one at 77 K and one at the substrate temperature, surround the sample

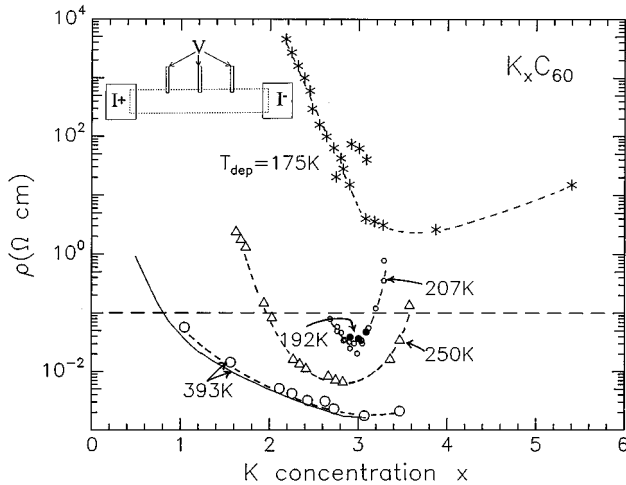


FIG. 1. Composition dependence of resistivity for K_xC_{60} codeposited at various substrate temperatures (ρ measured at 175 K for $T_{\text{dep}} \leq 250$ K and at 393 K for $T_{\text{dep}} = 393$ K). Dashed curves through data are guides to the eye. Samples with ρ below the horizontal dashed line show at least an onset to superconductivity. Solid curve indicates $\rho(x)$ for a sample grown at 393 K by the standard, sequential technique. Inset: schematic of sample (dashed line) and lead configuration for resistivity measurements.

space. The substrate temperature is determined by a calibrated Si-diode epoxied next to it. Thin-film thermometers ($T \geq 40$ K: Pt; $T \geq 40$ K; amorphous Nb-Si) deposited directly onto a few substrates indicate a temperature difference between the Si diode and the substrates of $\leq 2\%$ for $4 \text{ K} \leq T \leq 400 \text{ K}$ (with the radiation shields closed; when they are open during depositions above 77 K the difference increases to $\approx 2.5\%$); the Si-diode temperature is therefore used throughout this study. Calibrated crystal monitors for each source provide feedback for rate control and allow a determination of the film composition. Growth rates are $\sim 1.0 \text{ \AA/s}$. The films, ranging in thickness from 700 to 2000 \AA , are deposited onto prepatterned, 120- \AA -thick Pt voltage and current leads for dc four-probe resistance measurements (Fig. 1, inset). To ensure that the data represent 3D bulk properties, each codeposition is continued until the resistivity is independent of film thickness.

Figure 1 illustrates the resistivity ρ of K_xC_{60} as a function of x for different deposition temperatures during film growth, T_{dep} . T_{dep} controls the amount of disorder in the films, with greater disorder for films grown at lower T_{dep} . Each symbol depicts ρ (measured at 175 K for $T_{\text{dep}} \leq 250$ K and 393 K for $T_{\text{dep}} = 393$ K) of a different sample of average concentration x .¹³ For comparison between the standard growth technique, which can be used only at higher deposition temperatures, and the technique of codeposition used here, we also indicate ρ for a single sample (solid curve) grown at 393 K by first depositing 1000 \AA of C_{60} and subsequently doping with K. The resistivity is continuously monitored during K deposition. For increasing K concentration, ρ drops as the fraction of the metallic $x=3$ phase increases. The codeposited samples grown at $T_{\text{dep}} = 393$ K (open circles) closely track the solid curve, indicating that at high temperatures, films grown by the two techniques are similar, as expected.

At lower T_{dep} , ρ of all samples is higher than for samples grown at 393 K. For $T_{\text{dep}} \geq 192$ K there is a distinct minimum

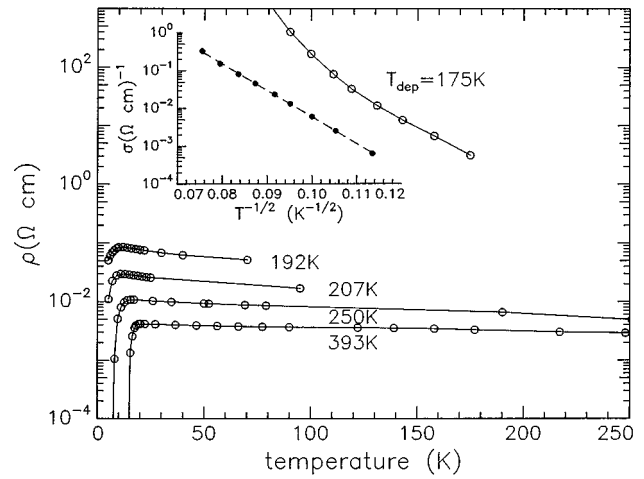


FIG. 2. Temperature dependence of resistivity of K_3C_{60} codeposited at various substrate temperatures. Inset: σ vs $T^{-1/2}$ for a sample grown at 175 K.

in $\rho(x)$ at $x \approx 3$. By $T_{\text{dep}} = 175$ K, ρ for $x \approx 3$ is more than 10^3 larger than in films grown at $T_{\text{dep}} = 393$ K; the variation of ρ with composition x is also qualitatively different than at higher deposition temperatures. At even lower T_{dep} , $\rho > 10^3 \text{ \Omega cm}$ ($T_{\text{dep}} \leq 77$ K; data not shown). The horizontal line at $\rho = 10^{-1} \text{ \Omega cm}$ indicates, to within a factor of 2, the value below which samples show at least an onset to superconductivity.

Concentrating on the samples with the lowest resistivity at each deposition temperature (i.e., $x \approx 3$), we display in Fig. 2 ρ as a function of measurement temperature for $175 \text{ K} \leq T_{\text{dep}} \leq 393$ K. As T_{dep} is lowered from 393 to 192 K, the magnitude of ρ increases, the superconducting onset temperature T_{onset} is reduced, and the transition width increases. For $T_{\text{dep}} \leq 175$ K, even samples with $x \approx 3$ are insulating. The inset to Fig. 2 shows that over the limited temperature range of measurement, the conduction follows the Efros-Shklovskii behavior for variable range hopping with strong electron correlations, $\sigma \propto \exp[-(T_0/T)^{1/2}]$.¹⁴ *In situ* reflection high-energy electron-diffraction (RHEED) measurements on K_3C_{60} indicate qualitatively that disorder is increased for lower T_{dep} yet with no dramatic structural differences between samples grown above and below 192 K. After high-temperature annealing, the $x \approx 3$ insulating samples recover their metallic and superconducting behavior while the $x \approx 6$ samples, with a filled conduction band, remain insulating, as expected (Fig. 3). Residual disorder is reflected in the lower T_{onset} and higher resistivity of the annealed $x \approx 3$ sample compared to those grown at high temperatures.

The transition from metallic to insulating behavior and T_{onset} track with the magnitude of the resistivity. The correlation is apparent in Fig. 4, where $\rho(T)$ is plotted for all samples, irrespective of concentration or deposition temperature. Data from Fig. 2 for samples with $x \approx 3$ are indicated by dashed lines. The Ioffe-Regel value for K_3C_{60} ($\sigma_{\text{IR}}^{-1} \approx 0.4 \text{ m\Omega cm}$) indicates the resistivity corresponding to a mean free path l equal to an intermolecular spacing, such that $k_F l = 2\pi$, where k_F is the Fermi wave vector.¹⁵ Note that samples with $\rho(20 \text{ K}) > 100 \times \sigma_{\text{IR}}^{-1}$ are still metallic and superconducting.

The experimental results in Figs. 1–4 can be summarized

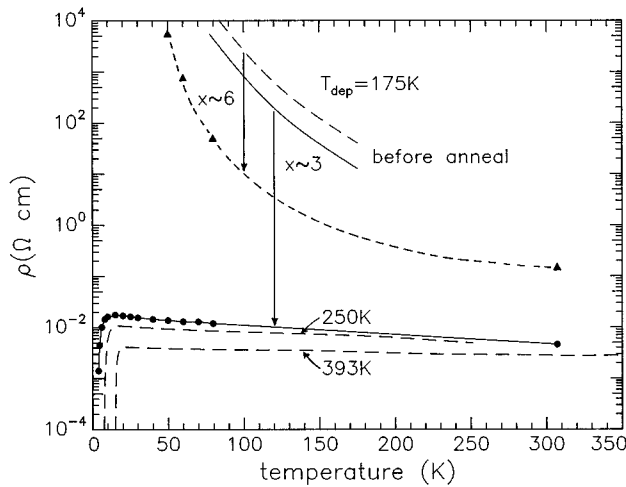


FIG. 3. $\rho(T)$ of K_xC_{60} samples ($x=3$, solid curve; $x\approx 6$, dashed curve) grown at $T_{\text{dep}}=175$ K before and after a 5 h anneal at 400 K. For comparison, data for K_3C_{60} grown at 393 and 250 K are also shown.

as follows. By reducing the film growth temperature, K_3C_{60} evolves from a superconductor into an insulator. Annealing the $x\approx 3$ disordered, insulating samples recovers the superconducting state.

These observations suggest that K_3C_{60} , a 3D metal at fixed composition, can be made insulating with increasing disorder. Conventional wide-band metals have a finite density of extended states at E_F , whether they are disordered or even amorphous. It appears that the conduction band in K_3C_{60} is sufficiently narrow and the electron density sufficiently small that disorder accompanied by correlations can completely alter the nature of the ground state of the system. This transition in K_3C_{60} is a striking example of the extreme sensitivity of alkali-doped C_{60} to disorder and correlations.

In 3D superconductor-semiconductor mixtures like amorphous Nb_xSi_{1-x} (Ref. 4) or in 3D superconductor-insulator mixtures,¹⁶ the concentration of a metallic component is the controlling variable for driving the transition. For these materials, a concentration range is always observed where the ground state is metallic [i.e., $\sigma(T\rightarrow 0)\neq 0$]. For K_xC_{60} , the transition can be driven in two ways, either by varying the disorder, the central result of this paper, or by varying composition. When disorder drives the transition, it appears that K_3C_{60} is either superconducting or insulating as $T\rightarrow 0$, with no intervening metallic state (Fig. 2). It has been predicted that 3D materials can undergo a direct transition from a superconducting to an insulating state.¹⁷ Additional experiments will be required, however, before we can rule out the possibility that K_3C_{60} has a metallic ground state with disorder intermediate to that in films grown at 175 and 192 K. When the concentration is varied away from $x=3$, the material also evolves from superconducting to insulating (Fig. 4, solid curves). A plot of $\sigma(T)$ suggests that samples with ρ at 4 K between 0.1 and 1 Ω cm are best fit with $\sigma_0+AT^{1/2}+BT$ with nonzero σ_0 , implying extended states at $T=0$ with no indication of superconductivity. Lower temperature measurements would however be needed to definitively conclude whether or not a metallic state is found between the superconducting and insulating states.

Two possible sources of the disorder driving this super-

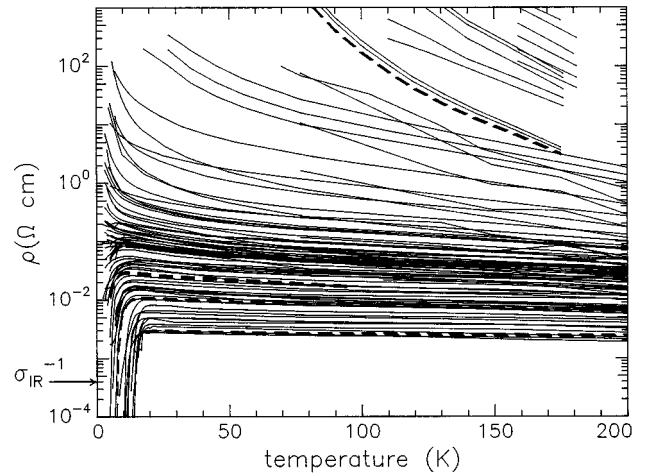


FIG. 4. $\rho(T)$ samples codeposited at several deposition temperatures and for many concentrations ($T_{\text{dep}}=393$ K: $1.1\leq x\leq 3.5$; 250 K: $1.6\leq x\leq 3.6$; 207 K: $2.4\leq x\leq 3.3$; 192 K: $2.9\leq x\leq 3.1$; 175 K: $2.2\leq x\leq 5.6$). Dashed curves: $x\approx 3$ (also shown in Fig. 2). σ_{IR} is the Ioffe-Regel value (Ref. 15).

conductor to insulator transition are grain boundaries and local defects, including in particular statistical fluctuations in the number of K ions neighboring each C_{60} . *Ex situ* x-ray measurements of C_{60} films grown on amorphous silicon nitride indicate that the grain size decreases from ≈ 300 Å for $T_{\text{dep}}=393$ K to ≤ 45 Å for $T_{\text{dep}}=77$ K. Transmission electron microscopy and RHEED data support this trend. The grain boundaries are the regions of maximum disorder, i.e., the regions where the electrons experience the maximum potential fluctuations. For a conventional wide-band metal, the potential fluctuations at grain boundaries are screened and act only as additional scatterers. However, in K_3C_{60} , with its narrow conduction band and low electron density, it is possible that electrons can be trapped at grain boundaries. K_3C_{60} may be similar to semiconductors with narrow impurity bands such as doped polycrystalline silicon, where electron traps at grain boundaries are a well-established phenomenon.¹⁸ Simple electron traps, however, might be expected to simply shift the minimum resistivity up from $x=3$. Granular K_3C_{60} films grown above room temperature by many research groups including ours have a relatively small temperature coefficient of resistivity, $d\rho/dT$, compared to the larger, positive $d\rho/dT$ of single-crystal data.¹⁰ This difference between large- and small-grained samples may be an initial indication of the destructive effects of disorder at the grain boundaries.

Alternatively, for lower T_{dep} , increased statistical fluctuations in local electron concentration could create superconducting and nonsuperconducting regions, despite an average $x=3$ composition. It is possible that in a disordered structure, incomplete charge transfer occurs, although this seems unlikely given the large electronegativity difference between K and C_{60} . Recent experiments on $Na_2Cs_xC_{60}$ and $A_{3-x}Ba_xC_{60}$ (A alkali) found that C_{60} with either two or four donated electrons per C_{60} are not superconducting, inconsistent with one electron band theory;¹⁹ ESR measurements suggest that they are weakly metallic with a low density of states.²⁰ We emphasize that the possibility that statistical fluctuations may

be important in K_3C_{60} is yet another indication of its unconventional nature. Aside from additional scattering, charge transport in conventional wide-band metals is insensitive to compositional fluctuations on a microscopic length scale. In the present case, where electronic length scales are so short ($\rho >$ Ioffe-Regel limit even for single crystal K_3C_{60} implies a mean free path $l < a_0$), it is not clear what microscopic length is required.

In conclusion, we have shown that for K_3C_{60} disorder is capable of driving a superconductor to insulator transition.

We speculate that due to its narrow conduction band and to electron correlations, K_3C_{60} shows a sensitivity to structural or chemical disorder which does not occur in conventional wide-band materials.

We gratefully acknowledge R. C. Dynes, S. Kivelson, J. Ostrick, L. Merchant, and members of the UCSD highly correlated-electron focus group for many insightful conversations, and K. Kavanagh for TEM measurements. This work was supported by NSF DMR-9208599.

-
- ¹For a review, see Patrick Lee and T. V. Ramakrishnan, *Rev. Mod. Phys.* **57**, 287 (1985).
- ²D. G. Naugle, *J. Phys. Chem. Solids* **45**, 367 (1984).
- ³J. M. Rowell and R. C. Dynes (unpublished).
- ⁴G. Hertel, D. J. Bishop, E. G. Spencer, J. M. Rowell, and R. C. Dynes, *Phys. Rev. Lett.* **50**, 743 (1983).
- ⁵For a review, see M. S. Dresselhaus, G. Dresselhaus, and P. C. Eklund, *Science of Fullerenes and Carbon Nanotubes* (Academic, San Diego, 1996).
- ⁶S. Saito and A. Oshiyama, *Phys. Rev. Lett.* **66**, 2637 (1991).
- ⁷R. W. Lof *et al.*, *Phys. Rev. Lett.* **68**, 3924 (1992); P. A. Brühwiler *et al.*, *Phys. Rev. B* **48**, 18 296 (1992); J. H. Weaver, *J. Phys. Chem. Solids* **53**, 1433 (1992); O. Gunnarsson, *Rev. Mod. Phys.* (to be published).
- ⁸S. Chakravarty and S. Kivelson, *Europhys. Lett.* **16**, 751 (1991).
- ⁹ K_3C_{60} is fcc with lattice constant 14.24 Å; three electrons per C_{60} ; Otto Zhou *et al.*, *Science* **255**, 833 (1992).
- ¹⁰A. F. Hebard *et al.*, *Phys. Rev. B* **48**, 9945 (1993); J. G. Hou *et al.*, *Solid State Commun.* **93**, 973 (1995).
- ¹¹V. J. Emery and S. A. Kivelson, *Phys. Rev. Lett.* **74**, 3253 (1995).
- ¹²O. Gunnarsson, E. Koch, and R. M. Martin, *Phys. Rev. B* **54**, R11 026 (1996).
- ¹³Absolute calibrations of the crystal monitors were determined from copper depositions. The minimum in ρ vs x occurs 10% below $x=3$ for $T_{\text{dep}}=393$ K and 10% above $x=3$ for 250 K $\geq T_{\text{dep}} \geq 192$ K. We assume this is an artifact of sticking coefficients which vary with substrate temperature and have multiplied the x values in Fig. 1 by 1.1 for $T_{\text{dep}}=393$ K and 0.9 for 250 K $\geq T_{\text{dep}} \geq 175$ K.
- ¹⁴A fit to $\sigma \propto \exp[-(T_0/T)^n]$ is slightly better for $n=1/2$ than for $n=1/3, 1/4$, or 1.
- ¹⁵A. F. Ioffe and A. R. Regel, *Semicond.* **4**, 237 (1960). Using $k_F l = 2\pi$, one finds $\sigma_{\text{IR}} = N^{1/3} e^2 / 1.5 h a_0$; a_0 is the lattice constant; N indicates the number of electrons per unit cell.
- ¹⁶See *Inhomogeneous Superconductors-1979*, edited by D. U. Gubser *et al.*, AIP Conf. Proc. No. 58 (AIP, New York, 1980).
- ¹⁷M. Ma and P. A. Lee, *Phys. Rev. B* **32**, 5658 (1985); A. Kapitulnik and G. Kotliar, *Phys. Rev. Lett.* **54**, 473 (1985).
- ¹⁸Ted Kamins, *Polycrystalline Silicon for Integrated Circuit Applications* (Kluwer, Boston, 1988).
- ¹⁹T. Yildirim *et al.*, *Phys. Rev. Lett.* **77**, 167 (1996).
- ²⁰T. Yildirim *et al.*, *Phys. Rev. B* **54**, 11 981 (1996).